Cellular Dynamical Mean Field Theory for the 1D Extended Hubbard Model

C. J. Bolech, S. S. Kancharla, and G. Kotliar

Center for Materials Theory, Serin Physics Laboratory, Rutgers University
136 Frelinghuysen Road, Piscataway, New Jersey 08854-8019, USA
(Dated: February 1, 2008)

We explore the use of exact diagonalization methods for solving the self consistent equations of the cellular dynamical mean field theory (CDMFT) for the one dimensional regular and extended Hubbard models. We investigate the nature of the Mott transition and convergence of the method as a function of cluster size as well as the optimal allocation of computational resources between bath and "cluster-impurity" sites, with a view to develop a renormalization group method in higher dimensions. We assess the performance of the method by comparing results for the Green's functions in both the spin density wave (SDW) and charge density wave (CDW) phases with accurate density matrix renormalization group (DMRG) calculations.

I. INTRODUCTION

The dynamical mean field theory (DMFT)[1] has been successful in accessing certain aspects of the non-perturbative phenomena in strongly correlated electron systems. For example, it has given new insights and predicted various qualitative trends in the redistribution of spectral weight as temperature, pressure and doping are varied in optical and photomission experiments, near the Mott transition.

Single site DMFT extracts physical quantities such as the self energy from a local impurity model with a self consistent bath (also refered to as LISA for local impurity self consistent approximation) and by construction this approach misses the effects of short range correlations, such as the k-dependence of the self energy, which are bound to become important at low temperatures. It also does not allow the treatment of phases such as d-wave superconductivity, and hence there have been significant efforts to extend the DMFT methodology[1,2,3,4,5,6,7,8].

Many of the elements of the DMFT method can be traced back to the coherent potential approximation (CPA)[9] which has been very successful in disordered systems. In this context, the search for extensions of the CPA was fraught with many difficulties, and extensions of DMFT should be scrutinized carefully in this light. The DMFT equations, while having a similar spirit to those of CPA for determining the effective medium, are considerably more complex because they involve the solution of a quantum impurity model, which plays the role of the effecive Hamiltonian for the local degrees of freedom treated in the DMFT. To analyse these equations new concepts and numerous techniques have been developed over the last decade. Their incorporation into cluster methods is promising but requires substantial new work. This paper is a contribution in this direction. In this paper we focus on one cluster extension of DMFT, the Cellular Dynamical Mean Field Theory (CDMFT)[5,10]. The aim of this paper is to investigate how the exact diagonalization aproach which was so successful in the context of the single site DMFT[11,12,13], can be used in the CDMFT context.

We solve the self consistent cluster equations for the one dimensional Hubbard and extended Hubbard models using exact diagonalization of the effective underlying cluster impurity. We choose these models because of their generic nature, as well as the fact that DMFT, which becomes exact in the limit of infinite coordination number[14], faces the worst case scenario in one dimension. Furthermore in one dimension fairly reliable computations of static as well as dynamic quantities can be made using the Density Matrix Renormalization Group (DMRG)[15,16,17] approach to carry out a comparative study.

The exact diagonalization approach, within the single site DMFT context, lead to the development of a technique inspired by renormalization group ideas which resulted in the first quantitative study of the critical properties near the Mott transition[18]. With a view towards the future, we discuss the possibility of combining renormalization group ideas and CDMFT to develop a new numerical method in the spirit of the DMRG.

The Extended Hubbard Model (EHM) is defined by the following Hamiltonian:

$$
\begin{aligned}
H = {} & -t \sum_{j,\sigma} \left(c^{\dagger}_{j+1\sigma} c_{j\sigma} + \text{h.c.} \right) + U \sum_j n_{j\uparrow} n_{j\downarrow} \\
& + V \sum_j n_j n_{j+1} - \mu \sum_j n_j
\end{aligned}
\tag{1}
$$

The first term corresponding to hopping between nearest neighbor sites and the second term to the onsite Coulomb repulsion provide the competition between itineracy and localization in the regular Hubbard model. The third term represents Coulomb repulsion between electrons occupying nearest neighbor sites. The Hamiltonian as written above with $\mu = U/2 + 2V$ guarantees an insulating ground state with a filling of one electron per site.

In the following section we introduce and discuss the CDMFT self consistency equations and show how they can be generalized to treat non-local Coulomb interactions even in the presence of broken symmetries. In the

next and subsequent sections we present results for the regular Hubbard and the extended Hubbard model respectively. This is followed by the conclusions and an outlook for further work.

II. THE CDMFT METHOD

The CDMFT[5] method is a straightforward generalization of the single site DMFT, in which local degrees of freedom within a cluster are treated exactly and those outside the cluster are replaced by a bath of non-interacting electrons determined self consistently. This approach, formulated with realistic studies in mind, deals in principle with overlapping cells and with clusters which are not necessarily defined in real space and could even be defined by non-orthogonal orbitals. In this paper, we ignore these complications and work with real space clusters using an orthogonal basis. It is worth pointing out, that if we apply the approach to non-interacting disordered alloys, the self consistency condition of CDMFT becomes identical to that used in the molecular CPA approximation of Ducastelle[19]. This is in the same way as the self consistency condition in single site DMFT becomes identical to the single site CPA and the two impurity approximation proposed by Ingersent and Schiller[20] and by Georges and Kotliar[1], becomes identical to the pair CPA. However, unlike the single site case, where the transition from real space to momentum space is unambiguous, one has to be careful in interpreting the results of the CDMFT equations in k-space. This is because the goal of CDMFT is to obtain the best possible estimates of *local* quantities that live within a cluster. For this purpose, it introduces a cluster self energy. Long distance properties such as the ones contained in the lattice Green's function and the lattice self energy are then *inferred* from the cluster Green's function or the cluster self energy while maintaining causality[5].

A. The Cavity Construction

The most economical way to arrive at the concepts of a dynamical mean field theory is via the cavity construction, which stresses the point made above, that the focus of the method is in extracting local quantities. The original lattice is divided into equal clusters of size N_c. Integrating out the degrees of freedom external to a chosen cluster (labelled 0), we can formally write an effective action which would allow the computation of local quantities as

$$\frac{1}{Z_{\text{eff}}}e^{-S_{\text{eff}}[c^{\dagger}_{0\mu\sigma},c_{0\mu\sigma}]} \equiv \frac{1}{Z}\int \prod_{j\neq 0,\mu\sigma}\mathcal{D}c^{\dagger}_{j\mu\sigma}\mathcal{D}c_{j\mu\sigma}e^{-S}. \quad (2)$$

Here j labels individual clusters and μ is an index labelling sites within each cluster. We can split the original

action into three parts,

$$S = S^{(0)} + S_0 + \Delta S, \quad (3)$$

where $S^{(0)}$ includes terms outside the chosen cluster (the full action with the cluster replaced by a cavity), S_0 comprises of terms solely within the cluster and finally, ΔS includes those terms that couple the cluster with its environment. Explicitly, in the case of the EHM,

$$\begin{aligned} S_0 &= \int_0^{\beta} d\tau \sum_{\mu\nu,\sigma\rho} c^{\dagger}_{0\mu\sigma}(\delta_{\mu\nu}\delta_{\sigma\rho}\partial_{\tau} + E^{00}_{\mu\nu,\sigma\rho})c_{0\nu\rho} \\ &\quad + \sum_{\mu}Un_{0\mu\uparrow}n_{0\mu\downarrow} + V\sum_{\langle\mu,\nu\rangle}n_{0\mu}n_{0\nu} \end{aligned} \quad (4)$$

$$\begin{aligned} \Delta S &= \int_0^{\beta} d\tau \sum_{\langle j\mu,0\nu\rangle,\sigma\rho} E^{j0}_{\mu\nu,\sigma\rho}c^{\dagger}_{j\mu\sigma}c_{0\nu\rho} + E^{0j}_{\nu\mu,\rho\sigma}c^{\dagger}_{0\nu\rho}c_{j\mu\sigma} \\ &\quad + V\sum_{\langle j\mu,0\nu\rangle}n_{j\mu}n_{0\nu} \end{aligned} \quad (5)$$

Here $\hat{E}^{00}$ includes the hopping matrix as well as the chemical potential within the zeroeth cluster and $\langle j\mu, 0\nu\rangle$ denotes all intercluster nearest neighbors. It is to be noted that, while the onsite Coulomb interaction U contributes only to S_0, a nonlocal interaction such as the nearest neighbor Coulomb repulsion V contributes to both S_0 as well as ΔS. This cavity construction is so far merely a relabelling of terms in the original action and is exact. However approximations need to be made to actually access the local properties within the cluster. We approximate the effective action of the cluster by keeping only the renormalization of the quadratic terms obtained after integrating out the degrees of freedom of the surrounding environment[1]. Notice that this approximation violates the translational symmetry of the original lattice. But this is not a problem, since the spirit of the approach is to estimate local quantities. The Gaussian approximation for the effects of the environment seen by the cluster becomes exact in the limit of large coordination[1] and therefore, our test case in one dimension constitutes the worst case scenario. The effective action for the cluster can then be approximated as,

$$\begin{aligned} S_{\text{eff}}\left[c^{\dagger}_{0\mu\sigma},c_{0\mu\sigma}\right] &= \int_0^{\beta} d\tau \sum_{\mu\nu,\sigma\rho} c^{\dagger}_{0\mu\sigma}\left[\hat{\mathcal{G}}_0^{-1}\right]_{\mu\nu,\sigma\rho} c_{0\nu\rho} \\ &\quad + \sum_{\mu}Un_{0\mu\uparrow}n_{0\mu\downarrow} + V\sum_{\langle\mu,\nu\rangle}n_{0\mu}n_{0\nu} \end{aligned} \quad (6)$$

Here, the time dependent Weiss field $\hat{\mathcal{G}}_0^{-1}$ is now a matrix in the cluster variables and is a functional of the EHM Green's function with the cluster replaced by a cavity. Suppressing spin indices, it can be written on the Mat-

subara axis as

$$\left[\hat{\mathcal{G}}_0^{-1}\left(i\omega_n\right)\right]_{\mu\nu} = i\omega_n\delta_{\mu\nu} - E_{\mu\nu}^{00} - V\,\delta_{\mu\nu}\sum_{\langle j\mu',0\nu\rangle}\langle n_{j\mu'}\rangle_{(0)}$$
$$- \sum_{\langle i\mu',0\mu\rangle}\sum_{\langle j\nu',0\nu\rangle}E_{\mu\mu'}^{0i}G_{i\mu',j\nu'}^{(0)}\left(i\omega_n\right)E_{\nu'\nu}^{j0}.$$

Relating the cavity Green's function, $G^{(0)}$, to the full Green's function of the EHM, the following self consistency condition to determine the Weiss field can be obtained:

$$\hat{\mathcal{G}}_0^{-1}(i\omega_n) = \hat{G}_{loc}^{-1}(i\omega_n) + \hat{\Sigma}_c(i\omega_n), \tag{7}$$

where the local Green's function on the cluster in one dimension is defined as (with an obvious generalization to higher dimensions)

$$\hat{G}_{loc}(i\omega_n) = \int_{-\pi/N_c}^{\pi/N_c}\frac{1}{i\omega_n + \mu - \hat{\Sigma}_c(i\omega_n) - \hat{t}(k)}\frac{dk}{2\pi/N_c}. \tag{8}$$

$\hat{\Sigma}_c$ is the cluster self energy as obtained from S_{eff}, $\hat{t}(k)$ is the Fourier transform of the cluster hopping matrix of the EHM and k is a vector in the reduced Brillouin zone of the superlattice $(-\frac{\pi}{N_c}, \frac{\pi}{N_c}]$. Explicitly for a one dimensional model with only nearest neighbor hopping,

$$t^{\mu\nu}(k) = -t[\delta_{\mu-\nu\pm1} + e^{-ikN_c}\delta_{N_c+\mu-\nu\pm1}$$
$$+ e^{ikN_c}\delta_{-N_c+\mu-\nu\pm1}] \tag{9}$$

B. A functional interpretation

A second approach to derive the above approximation is via the construction of a functional of the quantities of interest, say the Green's function restricted to a local cluster and its supercell translations, such that the stationary point of the functional yields those quantities[21]. In principle such a functional can be constructed order by order in a perturbative expansion in the hopping or the interactions while constraining the Green's function to a fixed value. In practice, sensible approximations to the exact functional are contructed by starting with the full Baym-Kadanoff functional $\Phi[G]$ and restricting its argument from the full Green's function to the Green's function defined only inside the cluster and its periodic supercell repetitions. This constraint is realized by the cluster self energy which plays the role of the Lagrange multiplier[21,22,23]. Differentiation of this functional gives the CDMFT equations. Viewed as an approximation to the Baym-Kadanoff functional for the full lattice, this procedure may seem a bad approximation[24]. However, this construction of the functional should be viewed as an approximation to the exact effective action for local quantities and CDMFT uses it precisely for such a purpose.

The functional approach is useful because it clarifies the level of approximation used in treating the broken symmetry state. In the case that we consider in this paper, all the Hartree graphs are added to the functional (see Eq. 11). The E-DMFT[6,8,21,25] includes additional graphs to the Hartree terms, but the quality of the results presented below show that they would make a very small contribution.

C. An Exact Diagonalization Algorithm

For the purpose of practical implementation of the algorithm it is convenient to consider the cluster effective action to arise from a generalized impurity Hamiltonian,

$$H_{imp} = \sum_{\mu\nu\sigma}E_{\mu\nu}c_{\mu\sigma}^\dagger c_{\nu\sigma} + U\sum_\mu n_{\mu\uparrow}n_{\mu\downarrow}$$
$$+ \sum_{\mu\nu}V_{\mu\nu}n_\mu n_\nu + \sum_{k\sigma}\epsilon_{k\sigma}a_{k\sigma}^\dagger a_{k\sigma}$$
$$+ \sum_{k\sigma,\mu}(V_{k\sigma,\mu}^h a_{k\sigma}^\dagger c_{\mu\sigma} + V_{k\sigma\mu}^{h*}c_{\mu\sigma}^\dagger a_{k\sigma}) \tag{10}$$

Here, $\epsilon_{k\sigma}$ represents the dispersion of an auxiliary noninteracting bath and $V_{k\sigma,\mu}^h$ is the hybridization matrix between the bath and the impurity cluster. The second and third terms include all the intra-cluster interaction terms. In $\hat{E}$ we lump together the cluster hopping matrix and chemical potential, as well as the Hartree terms arising from non-local interactions between clusters. For the EHM

$$E_{\rho\zeta} = E_{\rho\zeta}^{00} + V\,\delta_{\rho\zeta}\sum_{\langle j\rho',0\zeta\rangle}\langle n_{j\rho'}\rangle, \tag{11}$$

where $\langle n_{j\rho'}\rangle$ is computed by using the translational invariance of the system at the level of the superlattice.

In terms of the impurity model the parametrization of the Weiss field function is readily obtained as,

$$\hat{\mathcal{G}}_0^{-1}(i\omega_n) = i\omega_n - \hat{E} - \hat{\Delta}(i\omega_n); \tag{12}$$

where the hybridization function is given by

$$\Delta_{\mu\nu,\sigma}(i\omega_n)[\epsilon_{k\sigma}, V_{k\sigma,\delta}^h] = \sum_k\frac{V_{k\sigma,\mu}^{h*}V_{k\sigma,\nu}^h}{i\omega_n - \epsilon_{k\sigma}}. \tag{13}$$

Thus the algorithm involves determining the bath parameters $\epsilon_{k\sigma}$ and $V_{k\sigma,\mu}^h$ self consistently subject to the condition given by Eq. 7. Our implementation relies on the solution of the impurity model using exact diagonalization[11]. Starting with an inital guess for the bath parameters we obtain the cluster self energy $\hat{\Sigma}_c$, and using the self consistency condition determine a new Weiss field, $\hat{\mathcal{G}}_0^{-1}(i\omega_n)^{\text{new}}$. In turn, this defines a new hybridization function $\hat{\Delta}(i\omega_n)^{\text{new}}$. To close the self consistency loop we project onto a finite subspace of bath

size N_b. This projection is carried out using a conjugate gradient minimization of the following distance function,

$$D = \frac{1}{(n_{\max} + 1) N_b N_c} \sum_{n=0}^{n_{\max}} \left\| \hat{\Delta}(i\omega_n)^{\text{new}} - \hat{\Delta}(i\omega_n)^{N_b} \right\| \tag{14}$$

where $n_{\max}$ is the number of grid points on the Matsubara axis. Although we study the CDMFT equations only at zero temperature, the self consistency equations are solved on the Matsubara axis.

III. RESULTS FOR THE HUBBARD MODEL ($V = 0$)

In order to highlight the differences between the single impurity (LISA) and cluster dynamical mean field schemes we present results obtained for the local spectral gap as a function of the onsite Coulomb repulsion U. To keep the computational cost similar, we initially fix the total number of sites in the cluster and bath, $N_s = N_c + N_b = 6$, across schemes. The exact result for the gap is known from Bethe ansatz and is given by[26]

$$\Delta(U) = \frac{16t^2}{U} \int_1^{\infty} \frac{\sqrt{y^2 - 1}}{\sinh(2\pi t y / U)} dy \tag{15}$$
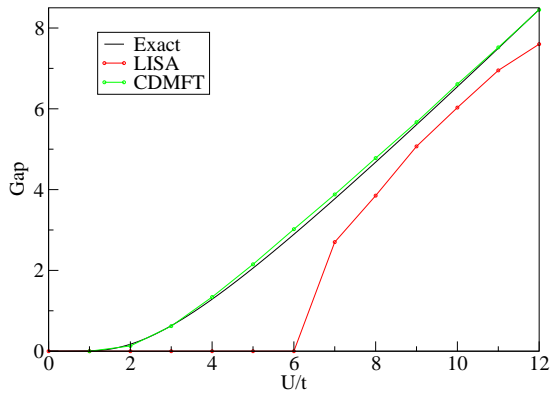

FIG. 1: Spectral gap as a function of U/t for the half filled Hubbard model.

Fig. 1 shows that there is a characteristically different behavior between the single impurity ($N_c = 1$) and cluster schemes ($N_c = 2$). In the single impurity case, for $U \gtrsim 7.5t$ the gap follows the exact result, whereas for $U \lesssim 7t$ it reduces to values much smaller than the exact gap and approaches zero. For the range $7t \lesssim U \lesssim 7.5t$ we observe a coexistence of the gapless and gapful phases. This transition from an insulating to a metallic phase is an artifact of the mean field approach which incorporates the physics of higher dimensions where the Mott transition is indeed present. On the other hand, CDMFT compares excellently to the exact gap and an insulating

solution exists through all finite values of U, in agreement with the well known physics of the one dimensional Hubbard model. We measure the half spectral gap as the point where the strength of the lowest frequency pole falls to 9% of its peak height. This percentage is arrived at by requiring that the gap at strong coupling be fixed at the exact value. We also find, as expected from the cavity construction and noted recently[24], that in the case of CDMFT, the bath only couples to sites on the boundary of the cluster, whereas for other cluster methods such as the dynamical cluster approximation (DCA) all the sites in the cluster are equivalently coupled to the bath. The self consistent procedure is robust and generates these two different kinds of solutions regardless of the nature of the starting guess.
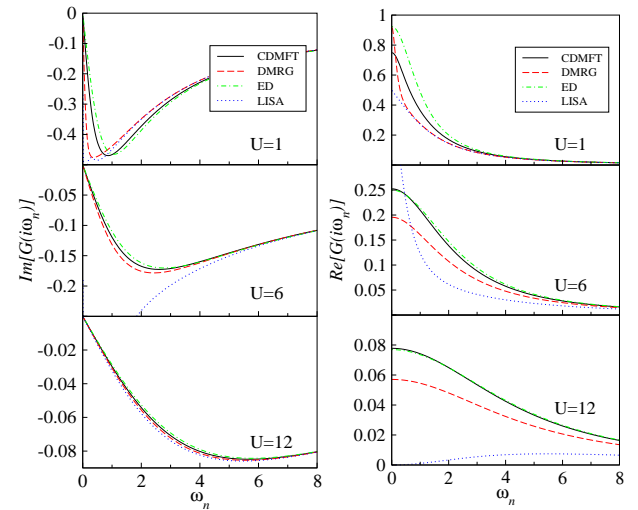

FIG. 2: Imaginary part of the onsite Green's function (left column) and real part of the nearest neighbor Green's function (right column) on the Matsubara axis for different values of U (in units of t).

To further illustrate the performance of the CDMFT method, in Fig. 2 we compare the onsite as well as nearest neighbor Green's functions on the Matsubara axis to those we obtain using the DMRG method. The calculation of dynamical correlation functions within the DMRG method is carried out by using the finite size algorithm[15] combined with the Lanczos vector method[16,17]. The results shown in the figures are those for chains with 18 sites and open boundary conditions. We verify that the results are close to those found by even longer chains and hence representative of the system in the thermodynamic limit. To highlight the role of the bath within the CDMFT method, we also overlay results obtained from exact diagonalization (ED) of a cluster of size $N_c = 2$, but without the bath. As U decreases we expect the difference between onsite Green's functions from the isolated cluster (ED) and the DMRG to increase, since the physics becomes less local. The contribution of the bath in CDMFT therefore becomes more significant with decreasing U and shows a systematic improvement with
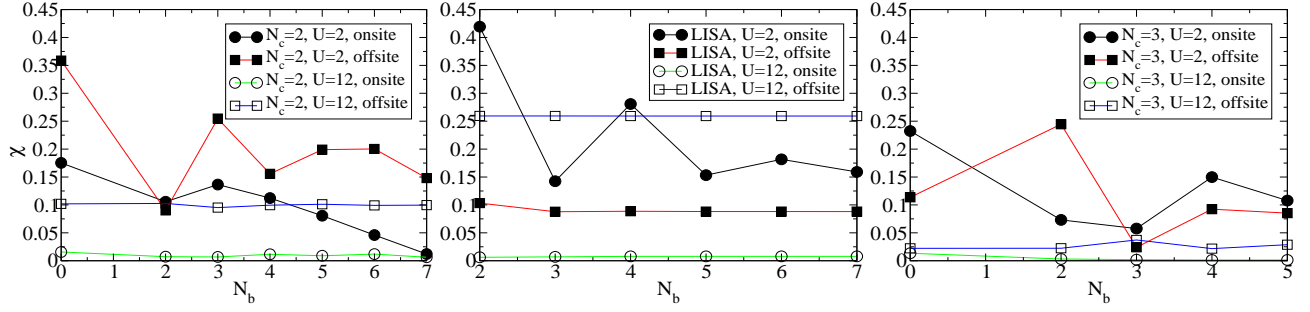
FIG. 3: Deviation of LISA and CDMFT Green's functions from the DMRG results as a function of the bath size N_b.

bath size as will be discussed later. Throughout the range of U we consider, the imaginary part of the onsite Green's function computed using CDMFT matches remarkably well with the DMRG curve. On the other hand a comparison for the real part of the nearest neighbour Green's function shows that the self consistent CDMFT solution achieves only a marginal improvement over the ED calculation for small U and almost none for large U. It can be clearly seen that the single impurity approach (LISA) performs poorly for the onsite Green's function for all U, except when U is large. Likewise, the nearest neighbor Green's function computed using LISA agrees poorly with the exact result throughout the entire range in U.

An important question to address is the issue of convergence and the nature of the self consistent solution as a function of the size of the effective impurity cluster and bath allotted in each case. In order to find a satisfactory self consistent solution, we find that the size of the Hilbert space allotted to the bath has to be at least comparable to that alloted to the cluster itself. For instance, clusters of size $N_c = 2$ require a minimum bath of size $N_b = 4$ for good convergence. Even and odd clusters show qualitatively different types of solutions, as we discuss further below. In Fig. 3 we plot χ, a measure of the deviation of the LISA and CDMFT solutions for the onsite and nearest neighbor Green's function from accurate results obtained using DMRG, as a function of the bath size N_b. This measure χ, is defined as the integrated absolute difference between the CDMFT (or LISA) and DMRG Green's functions.

Let us first discuss the results for the strong coupling case ($U = 12t$). The onsite Green's function computed using LISA compares excellently with DMRG and this continues to be so with the CDMFT method. There is practically no dependence of χ on the bath size. For the offsite Green's function, χ shows a systematic reduction with increasing cluster size, but remains fairly independent of the bath size.

For weak coupling, both LISA and CDMFT become exact. The toughest case is when U is of the order of the bandwidth; so in the following we discuss the results for $U = 2t$. For even clusters, we find that χ for the onsite Green's function shows a systematic decrease with increasing bath size once a minimum bath size is reached.

On the other hand, χ for the offsite Green's function shows no definite trend with increasing bath size.
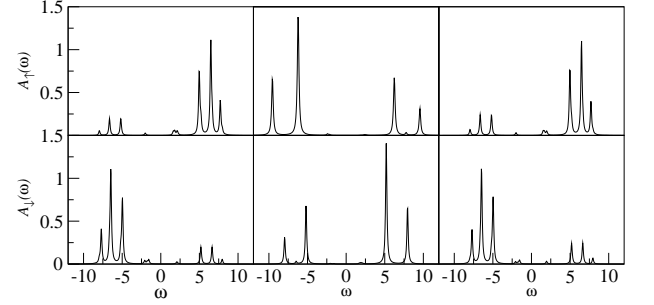

FIG. 4: From left to right we show the local spectral functions for sites one through three in a cluster of size $N_c = 3$. The bath size is fixed at $N_b = 6$.

Contrary to the expectations for a mean field solution, even cluster sizes ($N_c = 2, 4$) show no explicit local spin symmetry breaking. Odd clusters ($N_c = 3, 5$) show similar behavior for small bath sizes upto $N_b = N_c$. For larger bath sizes, $N_b \geq N_c$, and large enough U, the behavior of the local spectral function is spin dependent as can be seen from Fig. 4 for $U = 12t$. Odd clusters with broken symmetry are clearly inconsistent with cluster periodicty and consequently show poorer convergence. Thus, for all even clusters and odd clusters with small enough bath sizes, the one dimensional character of the problem is dominant over the role of the bath and prevents the self consistency from showing explicit spin symmetry breaking. On the other hand, odd clusters (we were able to test only the case $N_c = 3$) with large U and a sufficiently large bath show a symmetry broken solution consistent with the mean field approach.

The effect of the bath for $N_c = 3$ has an even more dramatic consequence at smaller U. As opposed to even clusters which correctly see only an insulating solution in one dimension, we see both a metallic and an insulating solution for $N_b \geq 5$ and $U \leq 3t$. In the region of coexistence, the metallic solution shows a better convergence than the insulating one. Thus, the improvement gained in going from LISA to $N_c = 3$ is that the region of coexistence moves to smaller U's and the insulating solution is present all the way upto $U = 0$. Small baths, due to the

absence of enough degrees of freedom to impose a mean field character to the solution, show an insulating state throughout the range in U. Beyond $N_c = 3$ for large enough odd clusters we expect to see only an insulating solution for all $U > 0$.
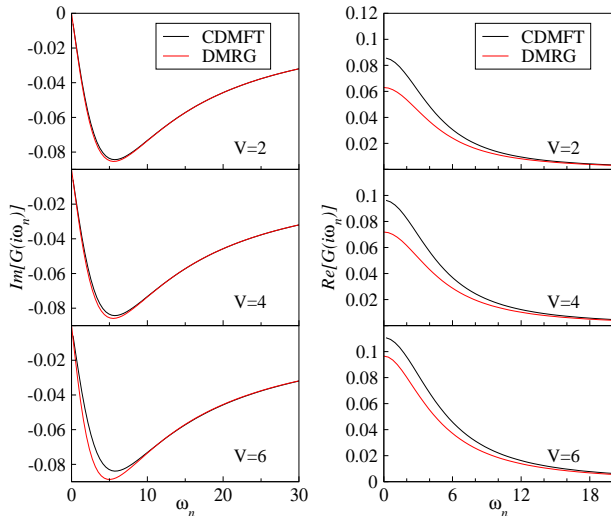
IV.   RESULTS FOR THE EHM ($V \neq 0$)

FIG. 5: Imaginary part of the onsite Green's function (left column) and real part of the nearest neighbor Green's function (right column) on the Matsubara axis for different values of V in the SDW phase.
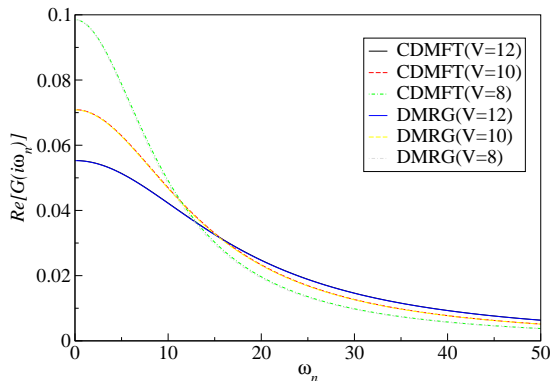
FIG. 6: Real part of the onsite Green's function in the CDW phase.

In this section we study the performance of cluster mean field methods as applied to the Extended Hubbard model. This model constitutes a natural test case since the non-local nearest neighbor Coulomb repulsion among different sites within the cluster can be accounted for exactly.

At half filling, for large enough U (strong coupling), the system goes through a first order transition from a spin
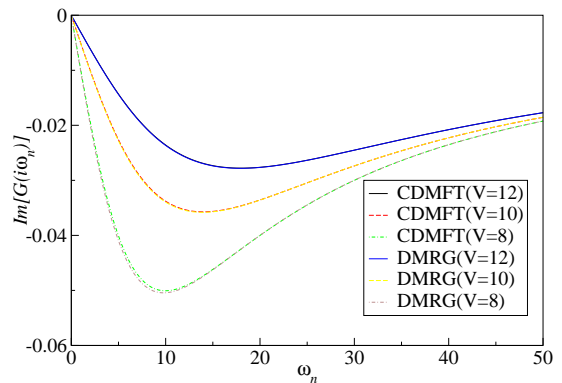
FIG. 7: Imaginary part of the onsite Green's function in the CDW phase.
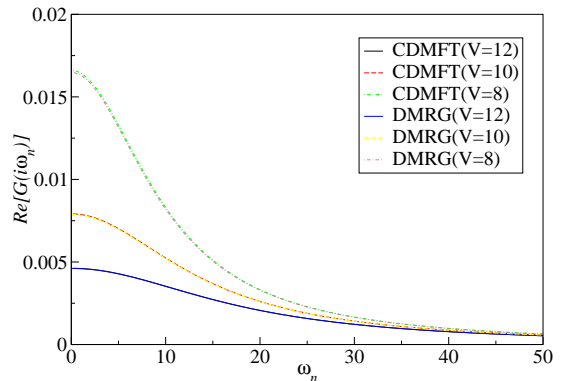
FIG. 8: Real part of the nearest neighbor Green's function in the CDW phase.

density wave (SDW) to a charge density wave (CDW) ordered state at roughly $V = U/2$[27,28,29]. We work in this regime, by fixing $U = 12t$ and scanning through the nearest neighbor Coulomb repulsion V. The CDMFT method shows a clear signature of this transition with a cluster as small as $N_c = 2$. In Fig. 5 we report a comparison of the imaginary part of the onsite Green's function and the real part of the near neighbor Green's function in the SDW phase. As seen in the $V = 0$ case, the comparison with DMRG is better for the former than the latter. We note that with increasing V the offsite Green's function compares better with the DMRG result. Figs. 6,7 and 8 compare the Green's functions within the CDW phase. Across the range in V, the agreement with DMRG is so remarkable that only one set of curves are discernable within the figures. In particular, Fig. 6 shows the real part of the onsite Green's function which is zero in the SDW phase but acquires a non-zero value in the CDW phase. This indicates a breaking of local particle-hole symmetry of the system that is now conserved only on the average every two sites. Notice how the curves for different values of V cross, defining a characteristic scale approximately equal to U. The versatility of CDMFT in being able to treat the ordered phase stems from the fact that it only assumes supercell periodicity and con-

sequently allows for complicated ordered states within a cell. This is in contrast to the DCA method that assumes full periodicity of the lattice, and therefore requires a fine discretization in momentum space to adequately capture the discontinuities in the Brillouin zone that appear with the emergence of short range ordered phases.
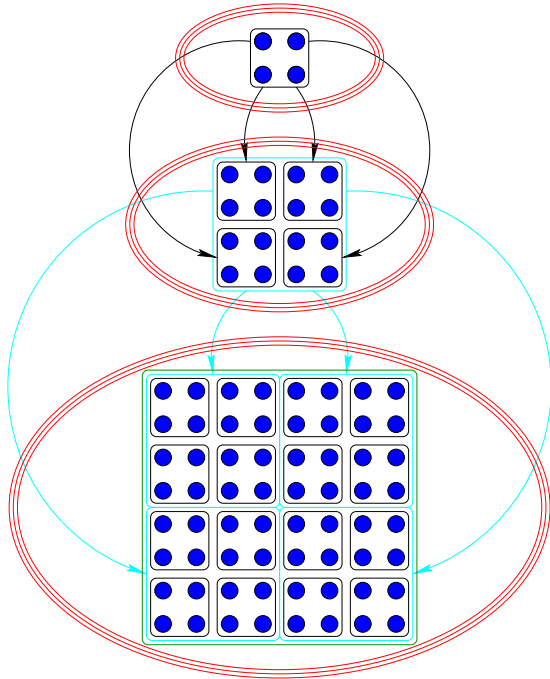
V. CONCLUSIONS AND OUTLOOK

FIG. 9: Schematic representation of an RG procedure intended to reach large cluster sizes.

We have shown that the CDMFT method produces remarkably good results when tested in one dimensional systems. This is very encouraging, since one would expect mean field methods to perform even better as the dimensionality increases. We saw that even the smallest possible cluster size ($N_c = 2$) along with a self consistent bath of modest size allows for an accurate determination of onsite correlations, while the offsite quantities improve systematically with increasing cluster size. Further, the success of our extension of the CDMFT equations to describe the discrete broken symmetry of the CDW order clearly demonstrates the power of the method to incorporate short range correlations.

Following the example of the EHM, with the simplest kind of short range correlation, it should be possible to treat the physics of more complicated ordered phases as well as unit cells of realistic materials within the cellular mean field approach. The main obstacle in this program is the computational effort that goes into solving the self consistent equations for the large clusters required by real world applications. This calls for a systematic approach

that blends together cluster dynamical mean field and renormalization group ideas[15,30] to select the most relevant degrees of freedom to represent a cluster.

We suggest that the CDMFT approach can be used iteratively in complete analogy with the density matrix renormalization group approach. It is useful to compare the similarities and differences between these two methods. In both of them, one improves on the exact diagonalization of a small finite size system by embedding the small system in a larger one; an embedding which can be described by a reduced density matrix. Within DMRG the density matrix is determined by an exact diagonalization of the larger system containing the subsystem of interest. In CDMFT, one can approximate the density matrix by modelling the enviroment with a Gaussian Weiss field.

The CDMFT assumption of a self consistent gaussian bath as the environment, that one can integrate out exactly in order to define a reduced density matrix for the cluster, becomes more and more accurate as the dimensionality increases. This choice of bath is optimum in a dynamical mean field sense (optimized for the computation of the local one particle Green's function of the cluster) and sidesteps the conventional DMRG procedure for building the reduced density matrix out of a few target states. Further, the DMRG prescription[15] of selecting the states for which the reduced density matrix has the largest eigenvalues allows for a truncation of the cluster Hilbert space while retaining the relevant physical information. In Fig. 9 we indicate schematically how such a method would proceed by doing CDMFT on small clusters, truncating their Hilbert space using the DMRG prescription and finally using them as building blocks of even larger clusters. This procedure can be repeated until either a desired cluster size or convergence in a certain observable of interest is reached. We believe this scheme should open new vistas for numerical renormalization group calculations of realistic systems in two and three dimensions.

APPENDIX A: DETERMINATION OF THE CLUSTER SELF ENERGY

The first step in the CDMFT iterative scheme is to compute the cluster self energy $\hat{\Sigma}_c$ for an initial guess of the bath parameters. This can be done using Eq. 7 by subtracting the inverses of the numerically determined cluster Green's function ($\hat{G}_{imp}(i\omega_n)$) from the exactly

known Weiss field. Although this is accurate enough for most purposes, when the results are small, it can introduce numerical errors. To deal with this, an alternative procedure was proposed in the context of the single impurity Anderson model[31]. The idea is to isolate contributions to the self energy coming purely from the hybridization and the interactions. The terms arising from the interactions can be written as ratios of correlation functions of composite operators leading to a more stable numerical procedure. We generalize this procedure to the cluster Anderson impurity model to write the self energy in the form

$$\hat{\Sigma}_c(i\omega_n) = \hat{\Sigma}_U(i\omega_n) + \hat{\Sigma}_V(i\omega_n) \tag{A1}$$

where

$$\Sigma_{U\sigma}^{\mu\nu}(i\omega_n) = U F_\sigma^{\mu\nu'}(i\omega_n) \left[\hat{G}_{imp}^{-1}\right]_\sigma^{\nu'\nu}(i\omega_n) \tag{A2}$$

$$\Sigma_{V\sigma}^{\mu\nu}(i\omega_n) = K_\sigma^{\mu\nu'}(i\omega_n) \left[\hat{G}_{imp}^{-1}\right]_\sigma^{\nu'\nu}(i\omega_n) \tag{A3}$$

and

$$F_\sigma^{\mu\nu} = \ll c_{\mu\sigma} c_{\mu\bar\sigma}^\dagger c_{\mu\bar\sigma}, c_{\nu\sigma}^\dagger \gg \tag{A4}$$

$$K_\sigma^{\mu\nu} = \sum_{\nu'} V_{\mu\nu'} \ll c_{\mu\sigma} n_{\nu'}, c_{\nu\sigma}^\dagger \gg$$

$$+ \sum_{\nu'} V_{\nu'\mu} n_{\nu'} \ll c_{\mu\sigma}, c_{\nu\sigma}^\dagger \gg \tag{A5}$$

Here $\ll A, B \gg$ denotes the Green's function of operators A and B. This method of computing the self energy is particularly robust for small values of U/t, when the self energy is relatively small in magnitude, as compared to the direct approach.

[1] For a review see A. Georges, G. Kotliar, W. Krauth and M. J. Rozenberg, Rev. Mod. Phys. **68**, 13 (1996)
[2] M.H. Hettler, A.N. Tahvildar-Zadeh, M. Jarrell, T. Pruschke, H.R. Krishnamurthy Phys. Rev. B **58**, R7475 (1998).
[3] S. Moukouri, C. Huscroft, and M. Jarrell, arXiv:cond-mat/0004279.
[4] A.I. Lichtenstein and M.I. Katsnelson, Phys. Rev. B **62**, R9283 (2000).
[5] G. Kotliar, S.Y. Savrasov, G. Palsson and G. Biroli, Phys. Rev. Lett. **87**, 186401 (2001).
[6] S. Pankov, G. Kotliar and Y. Motome, arXiv:cond-mat/0112083.
[7] S. Biermann, A. Georges, T. Giamarchi, A. Lichtenstein, arXiv:cond-mat/0201542.
[8] P. Sun and G. Kotliar, arXiv:cond-mat/0205522.
[9] R.J. Elliott, J.A. Krumhansl, P.L. Leath, Rev. Mod. Phys. **46**, 465 (1974).
[10] G. Biroli and G. Kotliar, Phys. Rev. B **65**, 155112 (2002).
[11] M. Caffarel and W. Krauth, Phys. Rev. Lett. **72**, 1545 (1994).
[12] M.J. Rozenberg, G. Moeller and G. Kotliar, Mod. Phys. Lett. B **8**, 535 (1994).
[13] Q. Si, M.J. Rozenberg, G. Kotliar, and A.E. Ruckenstein Phys. Rev. Lett. **72**, 2761 (1994).
[14] W. Metzner and D. Vollhardt, Phys. Rev. Lett. **62**, 324 (1989).
[15] S.R. White, Phys. Rev. Lett. **69**, 2863 (1992). S.R. White, Phys. Rev. B **48**, 10345 (1993).
[16] K.A. Hallberg, Phys. Rev. B **52**, 9827 (1995).
[17] T.D. Kuhner, S.R. White, Phys. Rev. B **60**, 335 (1999).
[18] G. Moeller, Q. Si, G. Kotliar, M. Rozenberg and D.S. Fisher, Phys. Rev. Lett. **74**, 2082 (1995).
[19] F. Ducastelle, J. Phys. C Sol. State. Phys. **7**, 1795 (1974).
[20] A. Schiller and K. Ingersent, Phys. Rev. Lett. **75**, 113 (1995).
[21] R. Chitra and G. Kotliar, Phys. Rev. Lett. **84**, 3678 (2000); Phys. Rev. B **63** 115110 (2001).
[22] R. Fukuda, M. Komachiya, S. Yokojima, Y. Suzuki, K. Okumura and T. Inagaki, Prog. Theory Phys. Suppl. **121**, 1 (1996).
[23] G. Kotliar Eur. Phys. J. B **11**, 27 (1999).
[24] T.A. Maier, O. Gonzalez, M. Jarrell, T. Schulthess, arXiv:cond-mat/0205460.
[25] J. L. Smith and Qimiao Si, Phys. Rev. B **61**, 5184 (2000).
[26] A.A. Ovichinnikov, Zh. Eksp. Teor. Fiz. **57**, 2137 (1969).
[27] M. Nakamura, Phys. Rev. B **61** 16377 (2000).
[28] S.S. Kancharla and C.J. Bolech, Phys. Rev. B **64**, 085119 (2001).
[29] F.H.L. Essler, F. Gebhard, and E. Jeckelmann, Phys. Rev. B **64**, 125119 (2001).
[30] K.G. Wilson, Rev. Mod. Phys. **47**, 773 (1975).
[31] R. Bulla, A.C. Hewson and T. Pruschke, J. Phys. Condens. Matter **10**, 83655 (1998).